Pergamon

0301-9322(95)00044-5

Int. J. Multiphase Flow Vol. 22, No. 1, pp. 19–30, 1996

0301-9322/96 $15.00 + 0.00

ENTRAINMENT AND DEPOSITION RATES IN A DISPERSED-FILM FLOW

R. I. NIGMATULIN[1], B. I. NIGMATULIN[2], YA. D. KHODZHAEV[2] and V. E. KROSHILIN[3]

[1]Tyumen Institute of Mechanics of Multiphase Systems (TIMMS), Ufa-Baskortostan Branch of the Russian Academy of Sciences, Moscow, Russia

[2]Research & Engineering Center of LWR Nuclear Plants Safety, Electrogorsk, Moscow oblast, Russia

[3]Institute of Mechanics, Moscow State University, Moscow, Russia

(Received 15 June 1993; in revised form 15 May 1995)

Abstract—Correlations and experimental data for entrainment and deposition rates in gas– or vapor–liquid dispersed-film (annular) flows have been considered and analyzed.

Key Words: dispersed-annular flow, droplet, onlet of entrainment, stabilized flow, surface tension, turbulent wall film thickness, volumetric droplet concentration

1. INTRODUCTION

Droplet moisture exchange is an important factor for heat- and mass-exchange processes of two-phase gas–liquid dispersed-film or dispersed-annular flows, whose behavior is determined by the distribution of mass flow between three components: gas or vapor ($m_1 = \frac{1}{4}\pi\rho_G^0\epsilon_1 v_1$), droplets in the flow core ($m_2 = \frac{1}{4}\pi\rho_L^0\epsilon_2 v_2$) and the wall film ($m_3 = \pi D\delta\rho_L^0 v_3$), where D is the inner tube diameter, δ is the averaged thickness of the liquid film ($\delta \ll D$), ρ_G^0 is the gas (steam) true density, ρ_L^0 is the liquid true density, ϵ_i is the volumetric gas ($i = 1$) or droplet ($i = 2$) concentration in the flow core ($\epsilon_1 + \epsilon_2 = 1$) and v_i is the average velocity of gas ($i = 1$), droplets ($i = 2$) or liquid in the film ($i = 3$). The droplet and gas velocities in the flow core are usually close to each other ($v_1 \approx v_2$) but the liquid velocity in the film is much lower than that of the gas or droplet velocity in the flow core ($v_3 \ll v_1$).

The mass flow rates m_1, m_2, m_3 change along the channel axis z according to the mass conservation equations (Nigmatulin 1991) for stationary flow:

$$\frac{dm_1}{dz} = J_{21} + J_{31},$$

$$\frac{dm_2}{dz} = -J_{21} + J_{32} - J_{23},$$

$$\frac{dm_3}{dz} = -J_{31} - J_{32} + J_{23}. \qquad [1]$$

Here J_{21} and J_{31} are the rates of evaporation of the droplets (2→1) and the film (3→1), respectively, J_{23} and J_{32} are the rates of droplet deposition on the film (2→3) and droplet entrainment (3→2) per channel length unit and per time unit, respectively.

Partial mass flow rates m_i and whole mass flow rate m for the mixture divided by channel cross-section will be denoted as mass fluxes and designated as m_i^0 and m^0, respectively:

$$m_i^0 = \frac{m_i}{\pi D^2/4} \quad (i = 1, 2, 3); \quad m^0 = \frac{m}{\pi D^2/4};$$

$$m = m_1 + m_2 + m_3, \quad m^0 = m_1^0 + m_2^0 + m_3^0 \qquad [2]$$

Further, this paper deals with experimental data known to the authors and the appropriate equations for J_{23} and J_{32}.

2. DROPLET DEPOSITION RATE

The deposition rate can be expressed by the droplet cross velocity w_{23} to the wall film, or by its ratio to the longitudinal velocity $v_1 \approx v_2$ which determines the non-dimensional deposition parameter J_{23}^*:

$$J_{23} = \pi D \rho_L^0 \epsilon_2 w_{23} = \pi D \rho_L^0 \epsilon_2 v_1 J_{23}^* \quad \left(J_{23}^* = \frac{w_{23}}{v_1} \right). \tag{3}$$

The deposition rate depends on phase physical properties ($\mu_G, \mu_L, \rho_G^0, \rho_L^0, \Sigma$), the droplet (volumetric) content ϵ_2 and the droplet velocity ($v_2 \approx v_1$):

$$J_{23} = f(\epsilon_2, v_1, \mu_G, \mu_L, \rho_G^0, \rho_L^0, \Sigma) \tag{4}$$

where μ_G and μ_L are the dynamic viscosities of the liquid and gas phases, respectively, and Σ is the coefficient of surface tension.

A survey of the articles devoted to the study of droplet deposition rate on the film is given by McCoy & Hanratty (1977) and by Nigmatulin (1991).

Rachkov (1979) realized [4] for his experimental data (for steam–water flow) in the following non-dimensional form:

$$J_{23} = 0.1 \epsilon_2^{-0.16} \mathrm{Re}_1^{-0.12} f(\Phi) \tag{5}$$

$$f(\Phi) = \begin{cases} \Phi^{0.5}, & \text{if } \Phi \leqslant 1 \\ \Phi, & \text{if } \Phi > 1 \end{cases}$$

$$\Phi = 0.16 \left(\frac{\Sigma}{v_1 \mu_G} \right) \left(\frac{\mu_G}{\mu_L} \right)^{0.5} \left(\frac{\rho_G^0}{\rho_L^0} \right)^{0.26}, \quad \mathrm{Re}_1 = \frac{\rho_G^0 v_1 D}{\mu_G}$$

This correlation was acquired while processing the experimental data where ϵ_2 changed in the range ($0.005 < \epsilon_2 < 0.1$).

A disadvantage of this equation which should be mentioned is that [5] includes the $\epsilon_2^{-0.16}$ co-factor which represents the small value of ϵ_2 to a small degree. Though this co-factor change is small ($2.33 \div 1.44$) in the ϵ_2 range corresponding to this experiment ($0.005 \div 0.1$), and $\epsilon_2 \to 0$ boundary, which corresponds to a single droplet in the flow core, it gives a physically inaccurate result: $J_{23}^* = w_{23}/v_1 \to \infty$. However, this disadvantage is easy to correct by changing the co-factor $\epsilon_2^{-0.16}$ by a reasonable approximation such as $\sim 2.4(1 - 4\epsilon_2)$.

Nigmatulin (1991) gives the equation acquired by Kukharenko on the basis of the theoretical analyses of droplet behavior in a turbulent flow and processing the data of the experiments in unheated air–water and steam–water flows:

$$J_{23}^* = 1.2(1 - 7.5\epsilon_2)\Pi \tag{6}$$

$$\left(\Pi = \frac{t^{(\mu)} v^*}{D} \frac{v^*}{v_1}, \quad t^{(\mu)} = \frac{2a^2 \rho_L^0}{9\mu_G}, \quad \frac{v^*}{v_1} = 0.2\, \mathrm{Re}_1^{-0.125} \right),$$

where a is the average droplet radius in the flow core included in the Π parameter. This was calculated using the empirical correlation of Whalley (1978):

$$\frac{2a}{D} = \mathrm{Re}_1^{0.1}\, \mathrm{We}_1^{-0.6} \left(\frac{\rho_G^0}{\rho_L^0} \right)^{0.6}, \quad \mathrm{We}_1 = \frac{\rho_G^0 v_1^2 D}{\Sigma}, \tag{7}$$

where We_1 is the Weber number for the flow determining the droplet size.

As a result, we get the following equation:

$$J_{23}^* = 9.6 \times 10^{-3}(1 - 7.5\epsilon_2)\mathrm{Re}_1^{0.95}\, \mathrm{We}_1^{-1.2} \left(\frac{\rho_G^0}{\rho_L^0} \right)^{0.2}. \tag{8}$$

As opposed to [5], [6] and [8] were acquired on the basis of the process mechanism analysis and can therefore be turned "semi-theoretical".

As distinct from [5] and [6], which take into account the influence of the gas and droplet velocity in the flow core $v_2 \approx v_1$ on the deposition rate, Hewitt & Govan (1990) suggested an equation in

their work which did not take into account this influence. The rate is only calculated from the relative droplet mass content ρ_2^*. This is why, in short, this equation can be denoted a "non-velocity" one. In this case another non-dimensional parameter J_{23}^{**} is used for the deposition rate with the help of parameter w_Σ having the velocity unit:

$$J_{23} = \pi D \rho_G^0 w_\Sigma \rho_2^* J_{23}^{**}, \qquad [9]$$

$$J_{23}^{**} = \begin{cases} 0.18, & \text{if } \rho_2^* < 0.3 \\ 0.083(\rho_2^*)^{-0.65}, & \text{if } \rho_2^* > 0.3 \end{cases}$$

$$\left(J_{23}^{**} = \frac{w_{23}}{\Sigma}, \quad w_\Sigma \equiv \sqrt{\frac{\Sigma}{\rho_G^0 D}}, \quad \rho_2^* = \frac{\epsilon_2 \rho_L^0}{\epsilon_1 \rho_G^0} \approx \epsilon_2 \frac{\rho_L^0}{\rho_G^0} \right).$$

Comparing it with [5] and [8], this Hewitt & Govan correlation can be presented, taking into account $J_{23}^* \equiv J_{23}^{**}(w_\Sigma/v_1) \equiv J_{23}^*(\mathrm{We}_1)^{-0.5}$, as:

$$J_{23}^* \equiv J_{23}^{**} \frac{w_\Sigma}{v_1} = \begin{cases} 0.18(\mathrm{We}_1)^{-0.5}, & \text{if } \rho_2^* < 0.3 \\ 0.083(\rho_2^*)^{-0.65}(\mathrm{We}_1)^{-0.5}, & \text{if } \rho_2^* > 0.3 \end{cases} \qquad [10]$$

One should point out once more that although the non-dimensional deposition rate J_{23}^*, corresponding to the Hewitt & Govan correlation [9], depends on v_1 ($J_{23}^* \sim \mathrm{We}_1^{-0.5} \sim v_1^{-1}$) in the last equation, the corresponding dimensional deposition rate J_{23} does not depend on the velocity v_1 with respect to [9] and [3]:

$$J_{23} \sim v_1 J_{23}^* \sim (v_1)^0.$$

The authors did not have any access to the parameters (in particular m_1, m_2, m_3), which allow calculation of the velocity value in the flow core for the experimental points given in Hewitt & Govan (1990), which is why these points could not be processed through [6] and [7]. In particular, not knowing v_1 one cannot calculate $J_{23}^* = J_{23}^{**}(w_\Sigma/v_1)$ using the data for J_{23}^{**} available in Hewitt & Govan. However, for the experimental points of Rachkov (1979) for steam–water flows [the experiments were carried out in a vertical tube $D = 0.013$ m with pressures $p = 1 \div 10$ MPa; mass flow rates $m = (7 \div 27) \times 10^{-2}$ kg/s; $\epsilon_2 = 10^{-3} \div 10^{-1}$; $v_1 = 4 \div 105$ m/s] and the experimental points of Netunaev (1982) for air–water flows ($D = 0.013$ m and $D = 0.031$ m; $p = 0.18 \div 0.45$ MPa, $m_2 + m_3 = (20 \div 250) \times 10^{-2}$ kg/s; $v_1 = 2 \div 60$ m/s, $\epsilon_2 = 10^{-3} \div 10^{-1}$) the authors had all the parameter values ($m_1, m_2, m_3, D, \rho_G^0, \rho_L^0, p, T$). These parameters allowed calculation of the gas and droplet velocities in the flow core ($v_1 \approx v_2$) and the volumetric droplet concentration ϵ_2 for every regime (experimental point):

$$\epsilon_2 \approx \frac{m_2/\rho_L^0}{(m_1/\rho_G^0) + (m_2/\rho_L^0)}, \quad v_1 \approx v_2 \approx \frac{m_1}{(\pi D^2/4)\rho_G^0} \quad (\text{if } \delta \ll D). \qquad [11]$$

Then using the phase physical properties μ_G, μ_L, ρ_G^0, ρ_L^0, Σ and the experimental points of Rachkov (1979) and Netunaev (1982) it appeared possible to process using [5], [6] and [7] and to compare their equivalence [only for the points of Rachkov (1979) and Netunaev (1982)]. The results of the comparison are given in figure 1†. This figure shows the calculated values of the non-dimensional depositions rate $(J_{23}^*)_{cal}$ for three equations [figure 1(a) for [5], figure 1(b) for [8] and figure 1(c) for [9]) and the corresponding experimental values $(J_{23}^*)_{exp}$. It is evident that [5] describes the "native" experimental points for which it was chosen well, and also the points by Netunaev (1982) (excluding five points corresponding to a low flow rate which are outlined with a dashed line in figure 1).

Apparently, this is connected either with the unreliability of these point measurements or with the act that [5] poorly describes the deposition process for low flow rates $v_1 = 2.5$ m/s. The "semi-theoretical" [8] and "non-velocity" equations [9] show considerable deviation from experimental points and systematically understate J_{23}^* for Rachkov (1979) experiments with steam–water flows and overstate it for Netunaev (1982) experiments with air–water flows.

†Further on in the article the experimental data of different authors are designated with triangles (Rachkov 1978), squares (Netunaev 1982) and circles (Hewitt & Govan 1990) the solid triangles, squares and circles relating the experiments with steam–water flows and the open ones relating to air–water flows.

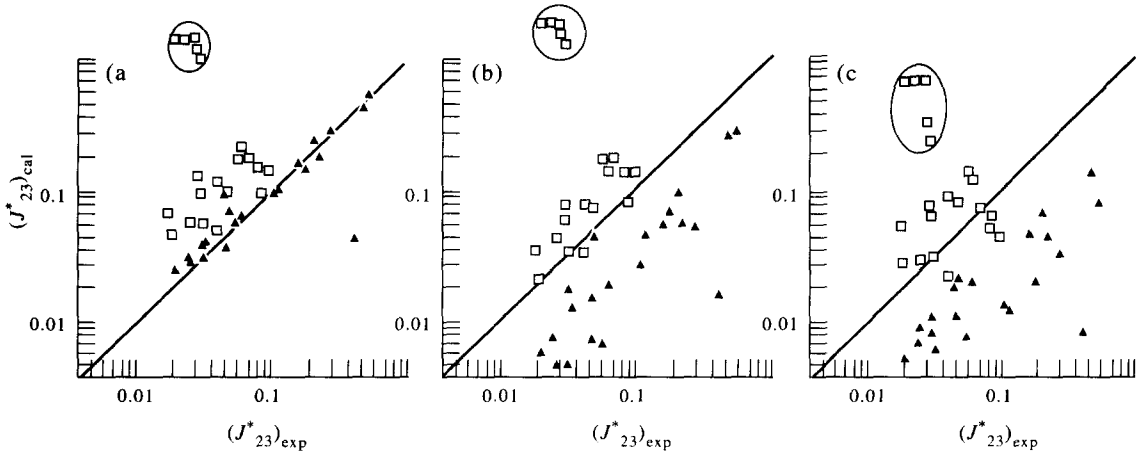

Figure 1. Comparison of correlations [5] by Rachkov (1979) (a), Kukharenko [6] (b) and Hewitt & Govan (1990) [9] (c) with the experimental data of Rachkov (1979) (▲, steam–water flows) and Netunaev (1982) (□, air–water flows) as regards the deposition rate J_{23}.

All three groups of experimental points can be analyzed and compared using non-dimensional variables J^{**}_{23} and ρ^*_2 used in Hewitt & Govan, which do not include the velocity v_1 (figure 2). It is evident now that [9] describes the "native" experimental points (Hewitt & Govan 1990) better than the "foreign" points (Rachkov 1979; Netunaev 1982), which are systematically higher than those of Hewitt & Govan (1990) and higher than the line corresponding to [9]. However, there is an important feature distinguishing [3] from [9], both always describing their "native" experimental points better than "foreign" ones. That is, the "non-velocity" equation [9] gives a considerable spread of values, not only for "foreign" points but also for "native" ones, as distinct from a very small spread given for its points by [5]. This is indicative of the redundant simplification of [7] connected with the fact that the influence of v_1 on droplet deposition is not taken into account.

Using the regime parameters of Rachkov's experiments (1979) mentioned above, we can analyze the influence of v_1 on the deposition rate J_{23} in these experiments. In figure 3(a) and (b) two groups of points are chosen. They differ in velocity v_1 only while the droplet mass content (ρ^*_2 or ϵ_2) and the physical phase properties remain fixed.

The relationship $J_{23}(d_1)$ integrating these experimental points is shown with a dash line. There are also three curves corresponding to [5], [8] and [9]. It is necessary to point out that the simple relationship $J_{23} = Cv_1^n$ corresponds to all three of these equations: for [5] $n = 0.38$ when $\Phi \leqslant 1$, and

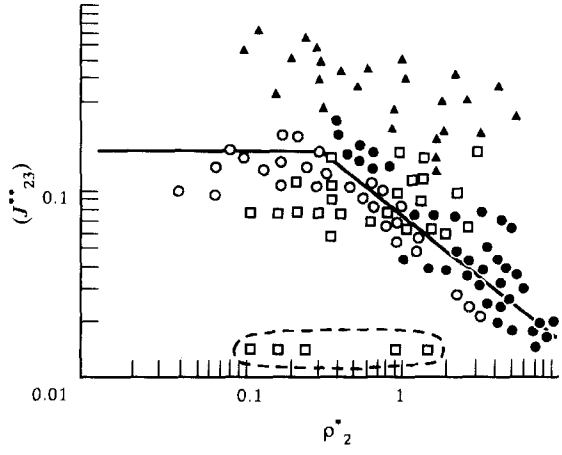

Figure 2. Comparison of the experimental points of Hewitt & Govan (1990) (●, steam–water flows; ○, air–water flows), Rachkov (1979) (▲, steam–water flows), Netunaev (1982) (□, air–water flows) using the correlation of Hewitt & Govan (1990) [9] for the deposition rate J_{23}. The solid broken line consisting of two straight pieces corresponds to [9].

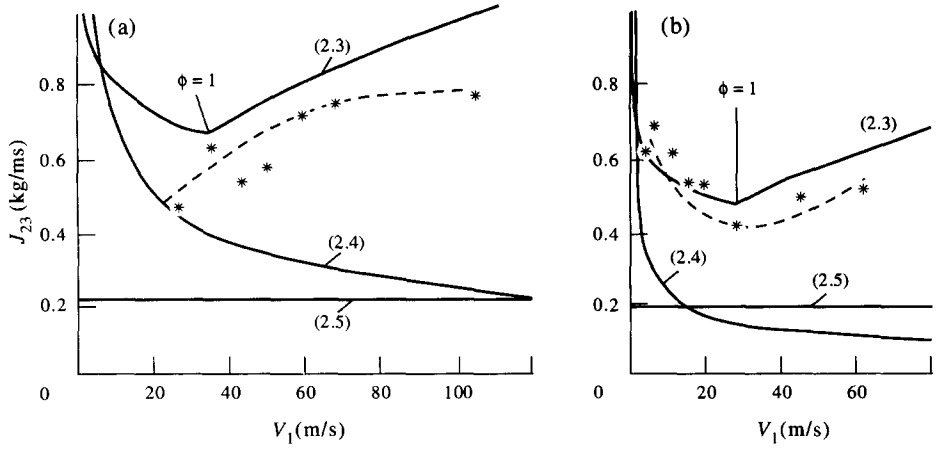

Figure 3. Dependence of droplet deposition rate on the flow velocity according to [5], [8], [9] and in the experiment. The dash line integrates the experimental points of Rachkov (1979).

$n = -0.12$ when $\Phi > 1$, i.e. $J_{23}(v_1)$ changes non-monotonously by v_1 for [6] $n = -0.45$ when J_{23} decreases with the growth of v_1; for [9] $n = 0$ when J_{23} does not depend on the velocity v_1.

It should be mentioned that in spite of the spread of the experimental points, v_1 noticeably influences J_{23}, and [5] covers this influence rather well. Yet this co-ordination should not be overestimated, as has already been stated, this equation is "native" for the experimental points shown in figure 3(a) and (b).

The structure of [8] (which is "more theoretical") than [5] and [9]) shows that, on the one hand, the increase of gas velocity v_1 leads to an increase of the gas velocity pulsation rate. This raises the probability of the droplet deposition rate. On the other hand, the increase of v_1 makes the size of the droplets entrained from the film become smaller. This reduces the probability of their coming back to the film. Additional experimental study is needed on the influence of the flow core velocity v_1, the turbulence rate, the size (mass) of the droplets, the surface tension Σ and droplet short-circuit on the deposition rate.

The analysis carried out and the comparison of the known studies in the field of droplet deposition rate on the liquid film surface allow the following to be concluded. When processed according to both [5] and [9], the experimental points of Rachkov (1979) and Netunaev (1982) are considerably higher than those of Hewitt & Govan (1990) [figures 1(a), (b) and 2].

Judging from the experimental points of Rachkov (1979), it is evident that only their "native" [5] describes them as well as the experiments by Netunaev (1982) (excluding 5 points). Equations [8] and [9] describe them much worse. However, additional experiments and analyses with more detailed information about the regime parameters are required in order to make a final judgement.

There is considerable scattering in three groups of experimental points (Rachkov 1979; Netunaev 1982; Hewitt & Govan 1990) for the variables [9] which can be explained by an unduly simplified description of deposition by [9], not taking into account the viscosity of the phases μ_G and μ_L or the gas velocity influence v_1.

We believe that the most promising way is to process the experiments on the basis of an equation of type [8] (with further modification) as that corresponding to a certain theoretical analysis of droplet behavior in a turbulent flow.

3. CONDITIONS OF ENTRAINMENT ONSET

Mainly in the works dealing with the determination of the critical conditions of the onset of dynamic entrainment at the surface by a gas flow, the experimentally determined critical or threshold gas velocity v_1 at which droplet entrainment from the film begins. A review of some of these works is given by Nigmatulin (1991).

Three correlative relations for the critical or threshold conditions of dynamic droplet entrainment from the film surface are analyzed below.

The increase of tangential tension τ_{13} on the film surface and increase of film thickness lead to entrainment onset. On the other hand, surface tension stabilizes the film surface and prevents entrainment onset.

So, it is natural to determine entrainment onset through a non-dimensional parameter, called the Weber number, for the film:

$$\mathrm{We}_{13} = \frac{\tau_{13}\delta}{\Sigma}. \qquad [12]$$

It is assumed that for turbulent flows $\tau_{13} \approx \rho_G^0 v_1^2$, and assumed that entrainment begins when

$$\mathrm{We}_{13} > \mathrm{We}_{13*}, \qquad [13]$$

where We_{13*} is the critical Weber number.

Nigmatulin *et al.* (1980) give the following equation (acquired by Rachkov) for the critical Weber number:

$$\frac{\mathrm{We}_{13*}}{(\mu_L/\mu_G)(\rho_G^0/\rho_L^0)^{1/2}} = \begin{cases} 2.5 \times 10^{-3}\,\mathrm{Re}_3^{0.2} & \text{when } \mathrm{Re}_3 \leqslant 300 \\ 2.8 \times 10^{-5}\,\mathrm{Re} & \text{when } \mathrm{Re}_3 > 300 \end{cases} \qquad [14]$$

$$\mathrm{Re}_3 = \frac{\rho_L^0 v_3 \delta}{\mu_L}.$$

The first approximation [14] corresponds to laminar films ($\mathrm{Re}_3 < 300$), and the second to turbulent films ($\mathrm{Re} > 300$). The tangential tension between the flow core and the film τ_{13} was determined from the pressure drop Δp measured in the experiment

$$-\Delta p \frac{\pi D^2}{4} - \tau_{13}\pi D + \rho g^z \frac{\pi D^2}{4} = 0 \qquad (\rho = \epsilon_1 \rho_G^0 + \epsilon_2 \rho_L^0), \qquad [15]$$

where ρ is the mixture density, g^z is the projection of the gravitation force on the pipe axis directed along the flow velocity v_1. For high-velocity flows the contribution of the second component in the right-hand side of [15] is usually negligible.

Though Δp was not measured in the course of the experiments, τ_{13} was calculated according to the following equation (Hewitt & Hall-Taylor 1972; Nigmatulin 1991; Whalley 1987):

$$\tau_{13} = \tfrac{1}{2} C_{13}\ \rho_G^0 (v_1 - v_{\Sigma 3})^2 \approx C_{13} \frac{\rho_G^0 v_1^2}{2} \qquad [16]$$

$$C_{13} = 0.005\left(1 + 168\left(\frac{2\delta}{D}\right)^{1.1}\right) \approx 0.005\left(1 + 120\frac{2\delta}{D}\right)$$

where $v_{\Sigma 3}$ is the liquid velocity on the film surface. It should also be borne in mind that usually $v_\Sigma \approx v_3 \ll v_1 \approx v_2$ for turbulent films. Equation [14] integrates the experimental data obtained under various conditions by many investigators. The accuracy is $\pm 20\%$ in concurrent air–water and steam–water flows in tubes when the pressure is $p = 0.1 \div 10$ MPa; $D = 10 \div 80$ mm (Figure 4).

Nigmatulin (1991) gives the following equation (acquired by Nikolaev) for entrainment onset:

$$\mathrm{We}_{13*} = \begin{cases} 8.5\bar{\mu}^{(\Sigma g)}, & \text{when } \mathrm{Re}_3 \leqslant 290; \\ 4.4 \times 10^{-3}\bar{\mu}^{(\Sigma g)}\mathrm{Re}_3^{4/3}, & \text{when } 290 \leqslant \mathrm{Re}_3 \leqslant 3 \times 10^3,\ g^z v_1 > 0; \\ 0.20 \times \bar{\mu}^{(\Sigma g)}\mathrm{Re}_3^{2/3}, & \text{when } 290 \leqslant \mathrm{Re}_3 \leqslant 3 \times 10^3,\ g^z v_1 > 0; \\ 5.5 \times 10^{-4}\,(\bar{\mu}^{(\Sigma g)})^{-0.75}, & \text{when } \mathrm{Re}_3 > 3 \times 10^3,\ g^z v_1 < 0; \end{cases} \qquad [17]$$

$$\bar{\mu}^{(\Sigma g)} = \mu_L \left(\frac{g}{\rho_L^0 \Sigma}\right)^{1/4},$$

where the first approximation corresponds to laminar ($\mathrm{Re}_3 < 290$) films, the second and the fourth to concurrent ($v_1 v_3 > 0$) turbulent ($\mathrm{Re}_3 > 290$) films in vertical ($g^z = \pm g$) upflows ($g^z v_1 < 0$) and the third to concurrent turbulent films in vertical downflows ($g^z v_1 > 0$).

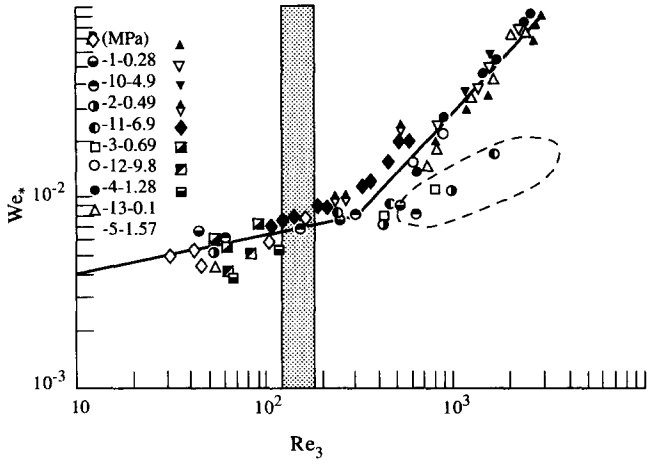

Figure 4. Results of experimental data processing of dynamic entrainment critical conditions for [14]: 1, ($p = 0.28$ MPa, $D = 9.5$ mm, air–water flows, upflow, Cousins *et al.* 1965); $2 \div 6$, ($p = 0.49 \div 4.41$ MPa, $D = 25$ mm, steam–water down flows, Mojarov 1950); $7 \div 12$, ($p = 0.98 \div 10$ MPa, $D = 13$ mm, steam–water up flows, Nigmatulin *et al.* 1982); $13 -$ ($p = 0.1$ MPa, $D = 26$ mm, air–water horizontal flows, Armand 1946); 14, ($p = 0.1$ MPa, $D = 79$ mm, air–water horizontal flows, Shevsky 1975; $15 \div 17$, ($p = 0.1 \div 0.45$ MPa, $D = 13$ and 31.5 mm, air–water up flows, Nigmatulin *et al.* 1982). The solid line of two straight segments corresponds to [14].

As compared to [13], Hewitt & Govan (1990) offer an essentially more simplified condition for droplet entrainment through the determination of the critical Reynolds number for the film:

$$\mathrm{Re}_3 > \mathrm{Re}_{3*}, \quad \mathrm{Re}_{3*} = \tfrac{1}{4}\exp\left[5.85 + 0.425\frac{\mu_G}{\mu_L}\left(\frac{\rho_L^0}{\rho_G^0}\right)^{0.5}\right]. \qquad [18]$$

The correlation equation [17] fundamentally differs from [14] and [18] by taking into account the gravity force vector influence with reference to the flow direction, so that the correlation equations differ for both upflows and downflows. In figure 4 the experimental points, corresponding to the downflow, are below those for the upflow. In connection with this, it is indicative that the influence of the gravity force direction, with reference to the flow velocity direction, [3.6] was set forward. This includes the gravity force acceleration value $\boldsymbol{g}$ and its direction with reference to the velocity v_1 ($\boldsymbol{g}^z v_1 > 0$; $\boldsymbol{g}^z v_1 < 0$). Later on, the authors noted that the experiments for downflows (and only for downflows unfortunate as it is) were carried out by Mojarov (1959).

Most of Mojarov's points (for downflows when $\mathrm{Re}_3 < 500$) correlate well with the corresponding experimental points of other authors (acquired for upflows), and only six or seven points (for downflows when $\mathrm{Re}_3 > 500$) are systematically lower than the main set of points for upflows. However, the estimation shows that for these points ($\mathrm{Re}_3 > 500$) the influence of gravity force must be small, as the corresponding parameter characterizing the gravity force influence is also small in comparison with the hydrodynamic forces:

$$\frac{\rho_L^0 g D}{\rho_G^0 v_1^2} = \left(\frac{\rho_G^0}{\rho_L^0}\mathrm{Fr}\right)^{-1} \ll 1, \quad \mathrm{Fr} = \frac{v_1^2}{gD} \qquad [19]$$

where Fr is the Froude number. This is why it is possible that the deviation of six or seven points from those of Mojarov (1959) can be explained by systematic error in the experiments corresponding to these points. In connection with this, [14] must be preferable from the point of view of physical validity to [17].

If this is so, the use of gravity force acceleration $\boldsymbol{g}$ in [17] is not justified in a physical sense, since $\boldsymbol{g} = 9.81$ m/s^2, as used in [3.6] does not reflect the gravity force influence. In particular, having conditions different from the Earth's does not mean that one should use a corresponding gravity force acceleration value which is different than 9.81 m/s^2. On the other hand, for experimental conditions with [17], this fault does not influence the agreement with the experimental points if we assume that $\boldsymbol{g}$ is a fixed number equal to 9.81 m/s^2.

Additional experimental research is needed to draw final conclusions about the influence of gravity force on droplet entrainment and its threshold conditions.

The threshold [18] corresponds to the dashed line in figure 4 ($Re_{3*} = 130 \div 190$). Evidently, the experimental points show that entrainment can occur when Re_3 is much lower then Re_{3*}. At the same time it may not occur when Re_3 is much higher than Re_{3*}. This fundamental disadvantage in [18] is a consequence of the fact that the equation does not take into account the surface tension Σ influence on the critical condition of entrainment though this influence is well-known from experiment and theory. This can particularly be seen in figure 4. In connection with everything mentioned above, [18] is unlikely to be promising as a description of the droplet entrainment threshold in a wide range of parameters.

4. DYNAMIC DROPLET ENTRAINMENT RATE

The dynamic droplet entrainment rate J_{32} can be represented through a non-dimensional value J_{32}^*:

$$J_{32}^* = J_{32}\frac{\pi D}{m_3} \qquad [20]$$

Nigmatulin *et al.* (1981) give the following function for a non-dimensional rate of dynamic droplet entrainment from the film surface:

$$J_{32}^* = \begin{cases} 0, & \text{if } We_{13} < We_{13*} \\ 91\,\dfrac{We_{13}}{Re_3}\left(\dfrac{\rho_L^0}{\rho_G^0}\right)^{\frac{1}{2}}, & \text{if } We_{13} > We_{13*} \end{cases} \qquad [21]$$

where We_{13*} is calculated according to [14]. The disadvantage of [21] lies in the non-continuous change of J_{32}^* when $We_{13} = We_{13*}$.

Nigmatulin (1991) gives the following function for a non-dimensional dynamic entrainment rate (as acquired by Nikolaev). This describes the physical entrainment process more consistently assuming that the more the Weber number We_{13} exceeds the critical value We_{13*}, the more the entrainment is†

$$J_{32}^* = 0.55\left(\frac{\rho_L^0}{\rho_G^0}\right)^{0.5}\frac{(We_{13} - We_{13*})^{0.85}}{(\bar{\mu}^{(\Sigma g)})^{0.7}\,Re_3} \qquad [22]$$

where We_{13*} is calculated according to [14] or [17]. As was already pointed out while discussing [17], a probable fundamental (but not influencing the agreement with the experimental points) disadvantage of this equation is the use of the fixed value of $g = 9.81\ m/s^2$ (for the $\bar{\mu}^{(\Sigma g)}$ parameter), which does not correspond to the gravity force influence.

Hewitt & Govan (1990) use another non-dimensional parameter for entrainment rate:

$$J_{32}^{**} = \frac{J_{32}D}{4m_1} = J_{32}^*\frac{m_3}{4\pi m_1} \qquad [23]$$

an an equation, which can be presented as follows, is offered:

$$J_{32}^{**} = \begin{cases} 5.75 \times 10^{-5}\Psi^{0.316}, & \text{if } Re_3 \geqslant Re_{3*} \\ 0 \end{cases}, \quad \text{if } Re_3 \leqslant Re_{3*} \qquad [24]$$

$$\left(\Psi = \frac{(Re_3 - Re_{3*})^2}{Lp_L}\left(\frac{\rho_L^0}{\rho_G^0}\right)^2;\quad Re_3 = \frac{\rho_L^0 v_3 \delta}{\mu_L} = \frac{m_3^0}{\mu_L};\quad Lp_L = \frac{\rho_L^0 \Sigma D}{\mu_L^2}\right).$$

In order to compare it with [21] and [22], this equation can be put in the following form:

$$J_{32}^* = 7.2 \times 10^{-4}\frac{m_1}{m_3}\left(\frac{\rho_L^0}{\rho_G^0}\right)\left(\frac{\delta}{D}\right)^{\frac{1}{2}}\left[\sqrt{We_3} - \sqrt{We_{3*}}\right]^{0.632}, \text{ if } We_3 > We_{3*}.$$

†In the book by Nigmatulin (1987) there is a misprint in this equation: instead of $\bar{\mu}^{(\Sigma g)}$ it should read $(\bar{\mu}^{(\Sigma g)})^{-0.7}$.

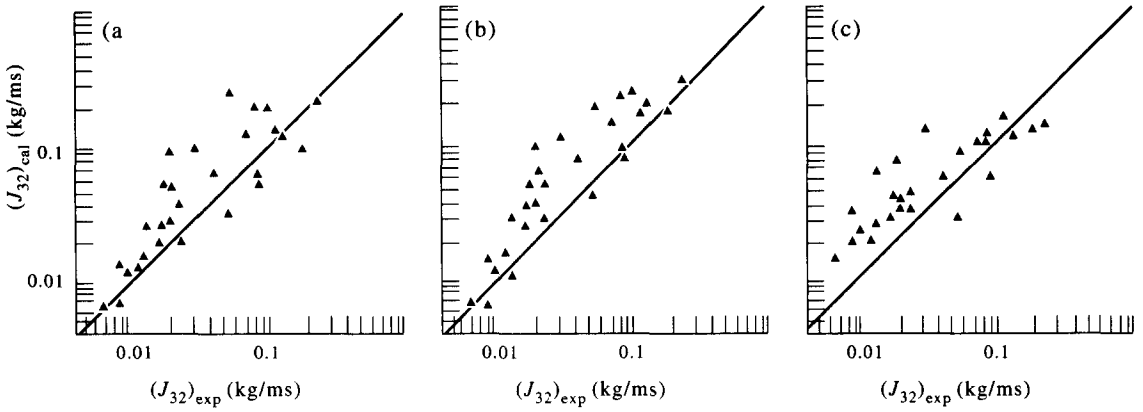

Figure 5. Comparison of correlations of Rachkov [21] (a), Nickolaev [22] (b) and Hewitt & Govan (1990) [24] (c) with the experimental data of Nigmatulin *et al.* (1981) (▲, steam–water flows) as regards the entrainment rate J_{32}.

$$\mathrm{We}_{3*} = \frac{\mathrm{Re}_{3*}^2}{Lp_L}\frac{D}{\delta}; \quad \mathrm{We}_3 = \frac{\rho_L^0 v_3^2 D}{\Sigma} = \frac{\mathrm{Re}_3^2}{Lp_L}\frac{D}{\delta}. \qquad [25]$$

Figure 5 shows the results of processing the experimental points of Nigmatulin & Rachkov (1981) for steam–water flows ($D = 0.0133$ m; $p = 1 \div 12$ MPa; $m = (6 \div 27) \times 10^{-2}$ kg/s; $x_1 = m_1/m = 0.2 \div 0.9$; $v_1 = 5 \div 125$ m/s) through [21] [figure 5(a)], [22] [figure 5(b)] and [24] [figure 5(c)]. The figures show that all the functions process the experimental data rather well.

Figure 6 shows the comparison of the experimental points of Nigmatulin *et al.* (1981) with the experimental points given by Hewitt & Govan (1990). As for the deposition not having the regime parameters ($m_1, m_2, m_3, \Delta p$) for the points of Hewitt & Govan (1990), it was impossible to process them in variables [20] and [21]. This is why, as in section 2, both groups of points (Nigmatulin *et al.* 1981; Hewitt & Govan 1990) were only processed and compared in coordinates [24]: J_{32}^*, Ψ. It is evident that the experimental data of both experimental groups match each other well in entrainment rate in contrast with deposition rate (figure 2).

It should be noted that Hewitt & Govan equations [23] and [24] include the liquid flow rate in the film m_3 determined by the product of v_3 by δ and do not include the velocity v_3 and the film thickness δ separately.

Equations [21] and [22] include the velocity v_3 and the film thickness δ separately which is, probably, more justified from the physical point of view, and thus more promising than [23] and [24]. Different thicknesses δ and velocities v_3 can be realized when the liquid mass flow rate

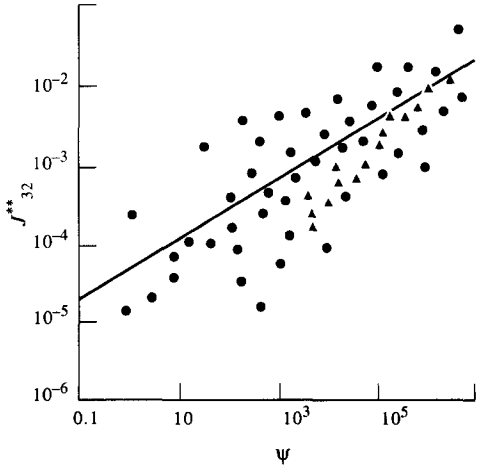

Figure 6. Comparison of the experimental points of Hewitt & Govan, (1990) (●, steam–water flows), Nigmatulin *et al.* (1981) (▲, steam–water flows) and the correlation of Hewitt & Govan (1990) [24] as regards the entrainment rate J_{32}. The solid line corresponds to [24].

($m_3 = \pi D \rho_l^0 \delta v_3$) in the film is fixed. This leads to different entrainment rates J_{32}: for a slowly moving thick film (low v_3 and high δ) and for a quickly moving thin film (high v_3 and low δ), when the mass flow rate m_3 is the same, entrainment rates must differ.

It should be mentioned that the velocity v_3 and the film thickness δ are determined by the mutual influence of the liquid film mass flow-rate m_3 stabilization due to entrainment and deposition and the velocity v_3 stabilization due to the friction force interaction of the film with the core flow and pipe wall.

5. ON THE STABILIZATION OF THE FILM VELOCITY, FILM THICKNESS AND LIQUID FLOW-RATE IN THE FILM

One of the principal methods of determining entrainment and deposition rates is that of measuring the liquid mass flow-rate in the film along the channel $m_3(z)$ and calculating dm_3/dz by means of numerical or graphical differentiation.

To determine the deposition rate J_{23} at the inlet of the measuring section ($z = 0$) all the liquid is supplied in the form of droplets, so at the beginning of the entrainment rate $J_{32} = 0$ because of the absence of the film ($m_3(0) = 0$). In this case J_{23} is determined by differentiation of the function $m_3 = m_3(z)$ at $z = 0$ or by the inclination of the corresponding line (line 1 in figure 7) at $z = 0$. Identically, to determine the entrainment rate J_{32} all the liquid at the inlet of the measuring section is supplied in the form of film, so that at the beginning of this section $J_{23} = 0$ because of the absence of droplets ($m_2(0) = 0$). The entrainment rate J_{32} is determined from the inclination of the linear section in the $m_3 = m_3(z)$ function at $z = 0$ (line 2 in figure 7). Thus, the determination of J_{23} and J_{32} is connected with numerical or graphical differentiation of the experimental function m_3 which increases the error.

The correlations [21] and [22] include the velocity v_3 and the liquid film thickness δ in addition to the liquid flow-rate in the film m_3, which is why, when [21] is used to process the experiments mentioned above, a problem arises as to how to specify δ or v_3 on the basis of the measured flow-rate ($m_3 = \pi D \rho_L^0 \delta v_3$) in the zone where J_{32} was measured. To determine the liquid film velocity v_3 and its thickness δ, some calculations were made for fixed values of the liquid film flow-rate m_3 at the inlet of the channel ($z = 0$), where all the liquid was concentrated in the film, but under different values of the liquid velocity v_3 in the film at the inlet ($z = 0$). The calculations showed that the measurement of the film thickness in the initial section is conditioned by two main mechanisms. The first mechanism is determined by the film friction forces on the flow core and wall, determining the velocity v_3. The second one is realized at the expense of droplet entrainment from the film. Figure 8(a) shows the comparison of experimental and calculated values of the liquid film flow-rate along the tube. The dotted line shows the values of equilibrium liquid flow-rate in the film (when the droplet entrainment is equal to the deposition). Figure 8(b) shows the calculated change of the liquid film velocity along the tube length (the dotted line shows the values of the film flow-rate of and equilibrium flow). The calculations were made according to the two-velocity

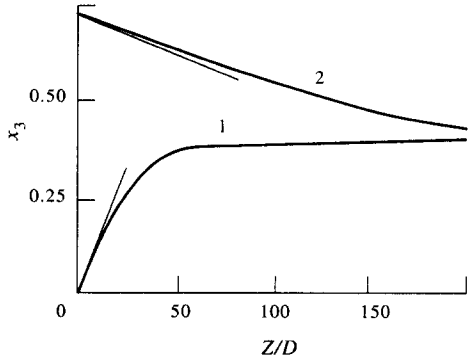

Figure 7. Characteristic change of liquid flow rate along the channel length from the channel inlet where all the liquid was supplied into the flow-core (line 1) or into the film (line 2) at a fixed pressure ($p = 69$ MPa, $D = 13.3$ mm, $m^0 = 1600$ kg/m^2 s, $x_1 = m_1/m = 0.27$, steam–water flow). Correlations [5] and [21] were used for calculations.

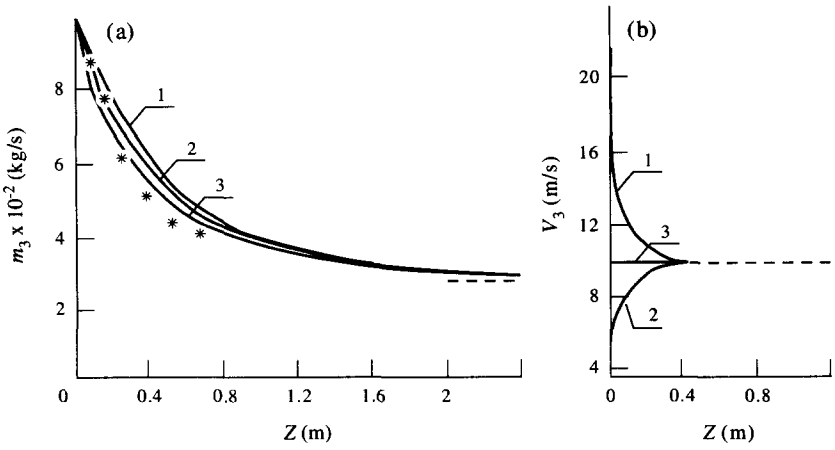

Figure 8. Comparison of the experimental (Nigmatulin *et al.* 1981) and calculated distributions along the tube (z-axis) of the liquid flow rate in the film $m_3(z)$ (a) and the calculated distribution of liquid velocity in the film v_3 (b) (steam–water flows: $p = 1.96$ MPa, $m^0 = 1220$ kg/m^2 s, $x = m_1/m = 0.4$) at the channel inlet ($z = 0$) when all the liquid at the channel inlet is supplied into the wall film ($m_2(0) = 0$, $x_3(0) = m_3(0) = 0.6$). Curves 1, 2 and 3 correspond to the values $v_{30} \equiv v_3(0) = 22.0$; 6.5 and 10.0 m/s.

annular dispersed model (see Nigmatulin 1991) taking into account the force and mass interactions between gas, droplets and film; in particular, [5] and [21] were used to calculate the deposition and entrainment rate. Figure 8(a) and (b) shows that the velocity in the film appears stable when $z < 0.3$ m, where the liquid mass flow-rate in the film m_3 changes linearly, in the first place, and, in the second place, does not have time to change significantly. That is, the stabilization of the velocity and the film thickness δ, at the expense of friction forces, runs rather quickly through a slowly changing liquid flow-rate in the film m_3 at the expense of entrainment and deposition. Two conclusions follow from this. First of all, the initial value of the liquid velocity v_3, supplied to the film at the inlet $z = 0$ and depending on the experimental device characteristic properties, does not have time to influence the film mass flow-rate m_3 change occurring at a much longer distance l_m than the distance l_v of stabilization v_3 ($l_m \gg l_v$). Secondly, to process entrainment experiments one may use the stabilized value of the film velocity $v_3 = (v_3)_{st}$ as it becomes stabilized in the zone $z < l_v \approx 0.3$ m (figure 7).

6. CONCLUSIONS

More detailed measurements of the critical conditions of entrainment, and entrainment and deposition rates are required in the future. They will allow development of accurate, reliable and physically and qualitatively valid equations for their determination.

Let us point out the conditions important for processing the results:

(1) It is impossible to obtain the equations for entrainment and deposition rates from theoretical hydromechanics. It is necessary to use qualitative ideas which should prompt empirical equation structure.

(2) The values of entrainment and deposition rate are acquired through numerical or graphical differentiation of the experimental data. This leads to error which can be decreased by increasing the number of experimental points and their accuracy.

(3) Entrainment and deposition are always simultaneous. Thus, the collisions of the depositing droplets with the near wall film surface cause additional entrainment of droplets from the film (shock spray entrainment). One should use numerical solutions (for experimental conditions) of mass and momentum conservation differential equations for the gas–droplet core and liquid film, making step-by-step revision of entrainment and deposition correlations using experimental data for liquid film flow-rate change along the channel.

REFERENCES

Armand, A. 1950 Hydraulic resistance of two-phase flow in horizontal tube. *Izv. Vses. Teplotech. Inst. Moscow* **1,** 16–23.

Cousins, L. B. & Hewitt, G. F. 1968 Liquid mass transfer in annular two-phase flow: radial liquid mixing. AERE-5693, England.

Hewitt, G. F. & Govan, A. 1990 Phenomenological modelling of non-equilibrium flows with phase change. *Int. J. Heat Mass Transfer* **33,** 229–242.

Hewitt, G. F. & Hall-Taylor, N. S. 1972 *Annular Two-phase Flow*. Pergamon Press, Oxford.

McCoy, D. D. & Hanratty, T. J. 1977 Rate of deposition of droplets in annular two-phase flow. *Int. J. Multiphase Flow* **3,** 319–331.

Mojarov, N. A. 1959 Research of the critical velocity of film entrainment from the pipe wall. *Thermal Energy* **2,** 50–53.

Netunaev, S. V. 1982 Gas–liquid medium modelling of local hydrodynamic characteristics of a steam–water flow. Ph.D. thesis, VNIIAM, Moscow.

Nigmatulin, B. I., Klebanov, L. A. & Kroshilin, A. E. 1980 Heat-transfer crisis for process steam-liquid dispersed anular flows under non-stationary conditions. *High Temp. Thermal Phys.* **18,** 1242–1251.

Nigmatulin, B. I., Rachkov, B. I. & Shugaev Y. A. 1981 Study of moisture entrainment rate from the liquid film surface in steam–water up flows. *Thermal Energy* **4,** 33–36.

Nigmatulin, B. I., Vinogradov, A. A. & Vinogradov, V. A. 1982 Methods of measuring the thickness and wave characteristics of the liquid film surface in a steam–water dispersed annular flow. *High Temp. Thermal Phys.* **20,** 6.

Nigmatulin, R. I. 1991 *Dynamics of Multiphase Media*, Vol. 2. Hemisphere, New York.

Rachkov, V. I., 1979 Experimental research of moisture-transfer processes in steam–water dispersed annular flows. Ph.D. thesis, Moscow.

Whalley, P. B., 1987 *Boiling, Condensation, and Gas–Liquid Flow*. Clarendon Press, Oxford.

Whalley, P. B., Hewitt, G. F. & Hutchi, P. 1973 Experimental wave and measurements in vertical annular two phase flow. AERE-R7521 UKAEA, Harwell, England.